elucidated the histological and biological characteristics of CD133$^+$ cells in non-neoplastic and neoplastic human livers.

Innovations and breakthroughs

Immunohistochemical analysis showed that CD133 was expressed constantly in the non-neoplastic biliary epithelium. In cholangiocarcinoma, CD133 was expressed diffusely in most carcinoma cells, whereas CD133$^+$ cells were identified in only a small number of cases of HCC. In combined carcinoma, most of the CD133$^+$ cells were CK19$^+$. In human HCC and cholangiocarcinoma cell lines, CD133$^+$ cells co-expressed CK19 or alpha-fetoprotein. CD133$^+$ or CD133$^-$ cells derived from human HCC and cholangiocarcinoma cell lines similarly could produce CD133$^+$ and CD133$^-$ progeny during subculturing, and there was no relationship between CD133$^+$ cells and the side population (SP) phenotype.

Applications

This study demonstrated that CD133 could be a biliary and progenitor cell marker *in vivo*. However, CD133 alone is not sufficient to detect tumor-initiating cells in cell lines. Theses results may provide insights into understanding the pathogenesis of various hepatobiliary diseases.

Terminology

CD133 (also known as prominin-1 or AC133) is a marker of hematopoietic progenitor cells. It has also been reported that CD133 is expressed in epithelial and non-epithelial progenitors in various tissues, in which the specific functions and ligands of CD133 have not been fully elucidated. SP is a minor population with extreme tumorigenic potential, and it is supposed that tumor-initiating cells exist in SP cells.

Peer review

The article presents interesting and novel data about CD133 expression in non-neoplastic and neoplastic liver tissues, and examines some biological characteristics of CD133$^+$ cells in HCC and cholangiocarcinoma cell lines. Although the authors presented some controversial data about the presence of CD133 expression in HCC, the experiments were designed appropriately, the methodology was precise, and the discussion supports the results.

REFERENCES

1 **Miraglia S**, Godfrey W, Yin AH, Atkins K, Warnke R, Holden JT, Bray RA, Waller EK, Buck DW. A novel five-transmembrane hematopoietic stem cell antigen: isolation, characterization, and molecular cloning. *Blood* 1997; **90**: 5013-5021

2 **Yin AH**, Miraglia S, Zanjani ED, Almeida-Porada G, Ogawa M, Leary AG, Olweus J, Kearney J, Buck DW. AC133, a novel marker for human hematopoietic stem and progenitor cells. *Blood* 1997; **90**: 5002-5012

3 **Shmelkov SV**, St Clair R, Lyden D, Rafii S. AC133/CD133/Prominin-1. *Int J Biochem Cell Biol* 2005; **37**: 715-719

4 **Uchida N**, Buck DW, He D, Reitsma MJ, Masek M, Phan TV, Tsukamoto AS, Gage FH, Weissman IL. Direct isolation of human central nervous system stem cells. *Proc Natl Acad Sci USA* 2000; **97**: 14720-14725

5 **Sagrinati C**, Netti GS, Mazzinghi B, Lazzeri E, Liotta F, Frosali F, Ronconi E, Meini C, Gacci M, Squecco R, Carini M, Gesualdo L, Francini F, Maggi E, Annunziato F, Lasagni L, Serio M, Romagnani S, Romagnani P. Isolation and characterization of multipotent progenitor cells from the Bowman's capsule of adult human kidneys. *J Am Soc Nephrol* 2006; **17**: 2443-2456

6 **Richardson GD**, Robson CN, Lang SH, Neal DE, Maitland NJ, Collins AT. CD133, a novel marker for human prostatic epithelial stem cells. *J Cell Sci* 2004; **117**: 3539-3545

7 **Oshima Y**, Suzuki A, Kawashimo K, Ishikawa M, Ohkohchi N, Taniguchi H. Isolation of mouse pancreatic ductal progenitor cells expressing CD133 and c-Met by flow cytometric cell sorting. *Gastroenterology* 2007; **132**: 720-732

8 **Ito Y**, Hamazaki TS, Ohnuma K, Tamaki K, Asashima M, Okochi H. Isolation of murine hair-inducing cells using the cell surface marker prominin-1/CD133. *J Invest Dermatol* 2007; **127**: 1052-1060

9 **Collins AT**, Berry PA, Hyde C, Stower MJ, Maitland NJ. Prospective identification of tumorigenic prostate cancer stem cells. *Cancer Res* 2005; **65**: 10946-10951

10 **O'Brien CA**, Pollett A, Gallinger S, Dick JE. A human colon cancer cell capable of initiating tumour growth in immunodeficient mice. *Nature* 2007; **445**: 106-110

11 **Ricci-Vitiani L**, Lombardi DG, Pilozzi E, Biffoni M, Todaro M, Peschle C, De Maria R. Identification and expansion of human colon-cancer-initiating cells. *Nature* 2007; **445**: 111-115

12 **Singh SK**, Clarke ID, Terasaki M, Bonn VE, Hawkins C, Squire J, Dirks PB. Identification of a cancer stem cell in human brain tumors. *Cancer Res* 2003; **63**: 5821-5828

13 **Singh SK**, Hawkins C, Clarke ID, Squire JA, Bayani J, Hide T, Henkelman RM, Cusimano MD, Dirks PB. Identification of human brain tumour initiating cells. *Nature* 2004; **432**: 396-401

14 **Suetsugu A**, Nagaki M, Aoki H, Motohashi T, Kunisada T, Moriwaki H. Characterization of CD133+ hepatocellular carcinoma cells as cancer stem/progenitor cells. *Biochem Biophys Res Commun* 2006; **351**: 820-824

15 **Yin S**, Li J, Hu C, Chen X, Yao M, Yan M, Jiang G, Ge C, Xie H, Wan D, Yang S, Zheng S, Gu J. CD133 positive hepatocellular carcinoma cells possess high capacity for tumorigenicity. *Int J Cancer* 2007; **120**: 1444-1450

16 **Ma S**, Chan KW, Hu L, Lee TK, Wo JY, Ng IO, Zheng BJ, Guan XY. Identification and characterization of tumorigenic liver cancer stem/progenitor cells. *Gastroenterology* 2007; **132**: 2542-2556

17 **Ma S**, Lee TK, Zheng BJ, Chan KW, Guan XY. CD133+ HCC cancer stem cells confer chemoresistance by preferential expression of the Akt/PKB survival pathway. *Oncogene* 2008; **27**: 1749-1758

18 **Sugawara H**, Yasoshima M, Katayanagi K, Kono N, Watanabe Y, Harada K, Nakanuma Y. Relationship between interleukin-6 and proliferation and differentiation in cholangiocarcinoma. *Histopathology* 1998; **33**: 145-153

19 **Goodell MA**, Rosenzweig M, Kim H, Marks DF, DeMaria M, Paradis G, Grupp SA, Sieff CA, Mulligan RC, Johnson RP. Dye efflux studies suggest that hematopoietic stem cells expressing low or undetectable levels of CD34 antigen exist in multiple species. *Nat Med* 1997; **3**: 1337-1345

20 **Chiba T**, Kita K, Zheng YW, Yokosuka O, Saisho H, Iwama A, Nakauchi H, Taniguchi H. Side population purified from hepatocellular carcinoma cells harbors cancer stem cell-like properties. *Hepatology* 2006; **44**: 240-251

21 **Fujii T**, Zen Y, Harada K, Niwa H, Masuda S, Kaizaki Y, Watanabe K, Kawashima A, Nakanuma Y. Participation of liver cancer stem/progenitor cells in tumorigenesis of scirrhous hepatocellular carcinoma--human and cell culture study. *Hum Pathol* 2008; **39**: 1185-1196

22 **Roskams TA**, Theise ND, Balabaud C, Bhagat G, Bhathal PS, Bioulac-Sage P, Brunt EM, Crawford JM, Crosby HA, Desmet V, Finegold MJ, Geller SA, Gouw AS, Hytiroglou P, Knisely AS, Kojiro M, Lefkowitch JH, Nakanuma Y, Olynyk JK, Park YN, Portmann B, Saxena R, Scheuer PJ, Strain AJ, Thung SN, Wanless IR, West AB. Nomenclature of the finer branches of the biliary tree: canals, ductules, and ductular reactions in human livers. *Hepatology* 2004; **39**: 1739-1745

23 **Haque S**, Haruna Y, Saito K, Nalesnik MA, Atillasoy E, Thung SN, Gerber MA. Identification of bipotential progenitor cells in human liver regeneration. *Lab Invest* 1996; **75**: 699-705

24 **Zen Y**, Fujii T, Yoshikawa S, Takamura H, Tani T, Ohta T, Nakanuma Y. Histological and culture studies with respect to ABCG2 expression support the existence of a cancer cell hierarchy in human hepatocellular carcinoma. *Am J Pathol* 2007; **170**: 1750-1762

25 **Theise ND**, Saxena R, Portmann BC, Thung SN, Yee H, Chiriboga L, Kumar A, Crawford JM. The canals of Hering and hepatic stem cells in humans. *Hepatology* 1999; **30**: 1425-1433

26 **Saxena R**, Theise N. Canals of Hering: recent insights and current knowledge. *Semin Liver Dis* 2004; **24**: 43-48

27 **Shmelkov SV**, Butler JM, Hooper AT, Hormigo A, Kushner J, Milde T, St Clair R, Baljevic M, White I, Jin DK, Chadburn A, Murphy AJ, Valenzuela DM, Gale NW, Thurston G, Yancopoulos GD, D'Angelica M, Kemeny N, Lyden D, Rafii S. CD133 expression is not restricted to stem cells, and both CD133+ and CD133- metastatic colon cancer cells initiate tumors. *J Clin Invest* 2008; **118**: 2111-2120

28 **Kim H**, Park C, Han KH, Choi J, Kim YB, Kim JK, Park YN. Primary liver carcinoma of intermediate (hepatocyte-cholangiocyte) phenotype. *J Hepatol* 2004; **40**: 298-304

29 **Zhang F**, Chen XP, Zhang W, Dong HH, Xiang S, Zhang WG, Zhang BX. Combined hepatocellular cholangiocarcinoma originating from hepatic progenitor cells: immunohistochemical and double-fluorescence immunostaining evidence. *Histopathology* 2008; **52**: 224-232

30 **Tickoo SK**, Zee SY, Obiekwe S, Xiao H, Koea J, Robiou C, Blumgart LH, Jarnagin W, Ladanyi M, Klimstra DS. Combined hepatocellular-cholangiocarcinoma: a histopathologic, immunohistochemical, and in situ hybridization study. *Am J Surg Pathol* 2002; **26**: 989-997

S- Editor Li LF **L- Editor** Kerr C **E- Editor** Ma WH

Multidrug resistance-associated protein 2 determines the efficacy of cisplatin in patients with hepatocellular carcinoma

PAVEL V. KORITA[1,2], TOSHIFUMI WAKAI[2], YOSHIO SHIRAI[2], YASUNOBU MATSUDA[3], JUN SAKATA[2], MASAAKI TAKAMURA[3], MASAHIKO YANO[3], AYUMI SANPEI[2], YUTAKA AOYAGI[3], KATSUYOSHI HATAKEYAMA[2] and YOICHI AJIOKA[1]

[1]Division of Molecular and Diagnostic Pathology, [2]Division of Digestive and General Surgery, and [3]Division of Gastroenterology and Hepatology, Niigata University Graduate School of Medical and Dental Sciences, 1-757 Asahimachi-dori, Chuo-ku, Niigata 951-8510, Japan

DOI: 10.3892/or_xxxxxxxx

Abstract. We hypothesized that expression of multidrug resistance-associated protein 2 (MRP2), a major cisplatin transporter, may determine the efficacy of cisplatin as a treatment for patients with hepatocellular carcinoma (HCC). A prospective analysis was conducted of 49 consecutive patients who underwent resection for HCC (16 patients treated with cisplatin-based neoadjuvant chemotherapy and 33 patients treated without neoadjuvant chemotherapy). Expression of MRP2 in resected specimens was assessed by immunohistochemical and Western blot analyses. The extent of tumor necrosis was assessed histologically in the greatest dimension of the tumor specimen from each patient. The median percentage of tumor necrosis was 81% (range: 0-100%) and complete tumor necrosis was found in 3 patients. Overexpression of MRP2 was detected in 24/46 (52%) tumor specimens. In 16 patients treated with cisplatin, tumor size and dose of cisplatin did not correlate with tumor necrosis of the resected specimens (P=0.706 and P=0.555, respectively). Of 13 tumor specimens containing vivid tumor from 16 patients treated with cisplatin, 8 had overexpression of MRP2. Tumor specimens with overexpression of MRP2 showed a lower percentage of tumor necrosis than those with non-overexpression (median percentage of tumor necrosis, 19% vs. 99%, P=0.003). In conclusion, overexpression of MRP2 correlates with a lower percentage of tumor necrosis in patients treated with cisplatin-based neoadjuvant chemotherapy for HCC, whereas either tumor size or dose of cisplatin does not. Expression of MRP2 determines the efficacy of cisplatin-based chemotherapy in patients with HCC.

Correspondence to: Dr Toshifumi Wakai, Division of Digestive and General Surgery, Niigata University Graduate School of Medical and Dental Sciences, 1-757 Asahimachi-dori, Chuo-ku, Niigata 951-8510, Japan
E-mail: wakait@med.niigata-u.ac.jp

Key words: hepatocellular carcinoma, drug resistance, multidrug resistance-associated protein 2, chemotherapy, cisplatin

Introduction

Multidrug resistance-associated protein 2 (MRP2; ABCC2), formally known as ATP-binding cassette (ABC), sub-family C, member 2, is a member of the superfamily of ABC transporters (1). MRP2 is localized to the canalicular (apical) membrane of hepatocytes (2-4), where it functions as a major exporter of organic anions, drugs, conjugated bilirubin, and bile salts to bile canaliculi (2-6).

MRP2 is one of the major transporters of cisplatin (7-9). *In vitro* experiments have shown that elevated expression of MRP2 decreases cisplatin accumulation in HCC cells and contributes to cisplatin resistance (9). Transfection of MRP2 antisense cDNA into a human hepatoma cell line decreased the MRP2 protein level and increased sensitivity to cisplatin (10). MRP2 expression in resected tumor specimens of patients with HCC, as detected by immunohistochemical analysis, ranges from 63 to 90% (11-13). In addition, MRP2 expression in tumor specimens is increased compared to non-neoplastic liver tissues using quantitative RT-PCR and Western blot analyses (13,14). The effect of tumor expression of MRP2 on the efficacy of cisplatin administration for patients with HCC has not been investigated previously. The aim of the current study was to test the hypothesis that expression of MRP2 may determine the efficacy of cisplatin-based neoadjuvant chemotherapy for patients with HCC.

Materials and methods

Patient population. From March 2007 through December 2008, a total of 59 consecutive Japanese patients with resectable HCC were referred to the Division of Digestive and General Surgery, Niigata University Medical and Dental Hospital (Niigata, Japan). Ten patients who received ablation therapy prior to surgical resection were excluded. The remaining 49 patients formed the basis of this prospective pilot study and included 39 men and 10 women with a median age of 70 years (range: 40-81 years). Signed informed consent

to participate in the current study was obtained from all patients. The current study was approved by the Institutional Review Board of Niigata University Medical and Dental Hospital.

Neoadjuvant chemotherapy. During the study period, neoadjuvant chemotherapy was applied to prevent tumor progression when a patient was on the waiting list for definitive operation for HCC for more than one month. The decision to use neoadjuvant chemotherapy was made by the Institutional Cancer Committee of Niigata University Medical and Dental Hospital. Indications for neoadjuvant chemotherapy included multiple hepatic tumors or a solitary tumor >3 cm in diameter, because these preoperative factors are closely associated with vascular invasion or poor post-resection survival (15-17). In the current series, 16 patients received neoadjuvant chemotherapy, which consisted of hepatic arterial infusion of a fine-powder formulation of cisplatin (IA-call®, Nippon Kayaku, Co., Ltd., Tokyo, Japan; recommended dose of 65 mg/m^2) under the guidance of hepatic angiography. The remaining 33 patients did not undergo neoadjuvant chemotherapy for HCC. The size of the largest hepatic tumor ranged from 1.5 to 12.1 cm (median tumor size, 3.5 cm) on contrast-enhanced spiral computed tomography (CT) images before neoadjuvant chemotherapy.

The response to neoadjuvant chemotherapy was assessed by contrast-enhanced spiral CT and was evaluated according to the Response Evaluation Criteria in Solid Tumors (RECIST) guidelines (18). Treatment-related toxicity was evaluated according to the Common Terminology Criteria of Adverse Events (CTCAE version 4.0; National Cancer Institute, Bethesda, MD, USA) (19).

Hepatectomy procedures. A hepatectomy procedure was selected for each patient, taking the primary tumor status (size, number, location), the hepatic functional reserve, and the patient's general condition into account (16). In the current study, the term 'major hepatectomy' indicated formal hemihepatectomy or more extensive resection, whereas less extensive hemihepatectomy was designated 'minor hepatectomy'. Postoperative morbidity was defined as any postoperative complication that lengthened the hospital stay (16).

Pathologic evaluation. Resected specimens were submitted to the Department of Surgical Pathology of Niigata University Medical and Dental Hospital. Each specimen was examined to determine the presence of cirrhosis, the number of hepatic tumors, the size of the largest hepatic tumor, the histologic grade, and gross or microscopic vascular invasion. The pathologic findings were described according to the TNM Classification of Malignant Tumours by the International Union Against Cancer (6th edition, 2002) (20).

A total of 90 hepatic tumors were resected in the current series. Twenty-eight patients had a solitary tumor and 21 had multiple tumors. The number of hepatic tumors was determined by gross examination of multiple slices from each resected specimen, but did not include satellite nodules. The definition of satellite nodules followed that of Taylor *et al* (21), regarding colorectal carcinoma liver metastasis. In patients with multiple tumors, the largest tumor was chosen as representative of all tumors.

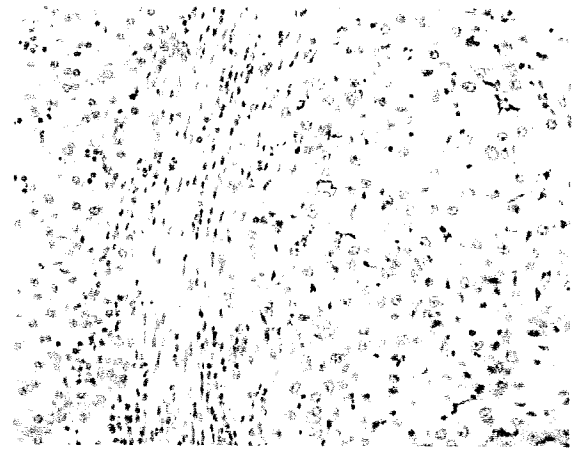

Figure 1. Hepatocellular carcinoma with overexpression of multidrug resistance-associated protein 2 (MRP2). Non-neoplastic hepatocytes in the left half show faint MRP2 expression in the canalicular membranes of hepatocytes, whereas cancerous tissue in the right half has overexpression of MRP2. Immunohistochemical staining: original magnification, x400.

The microscopic diagnosis of cirrhosis in the adjacent non-neoplastic liver was defined as the presence of regenerative nodules surrounded by fibrous septa. Using these criteria 33 patients had liver cirrhosis histologically verified. The median tumor size was 2.8 cm (range: 1.1-10 cm) in the resected specimens and the histologic grade was determined according to the Edmondson-Steiner classification (22), which is based on the areas of the tumor with the highest grade. Vascular invasion was defined as gross or microscopic involvement of the vessels (portal vein or hepatic vein) within the peritumoral liver tissue (17).

The extent of tumor necrosis was assessed histologically in the greatest dimension of the tumor specimen from each patient. The percentage of tumor necrosis was defined as the ratio between total necrotic area and the whole area of the tumor, multiplied by 100. In the greatest dimension of the tumor specimens from 16 patients who received neoadjuvant chemotherapy, the median necrotic area was 113.4 mm^2 (range: 0-2862 mm^2), whereas the median whole tumor area was 336.5 mm^2 (range: 57-5498 mm^2).

Immunohistochemistry. From each resected specimen, 1 to 3 paraffin-embedded block(s) (median, 2 blocks) were used for immunohistochemistry. Three serial 3-μm sections were re-cut and prepared from each block; 1 for hematoxylin and eosin staining, 1 for MRP2-immunohistochemical staining, and 1 as a negative control. Two independent surgical pathologists blinded to the clinical details assessed each section.

The streptavidin-biotin immunoperoxidase method was performed using the Histofine SAB-PO (M) kit (Nichirei Biosciences Inc., Tokyo, Japan). The sections were deparaffinized and rehydrated, then microwaved at 500 W for 7 cycles of 3 min in 10 mmol/l sodium citrate buffer (pH 6.0) to retrieve antigenic activity. Endogenous peroxidase activity was inhibited by incubation with 0.3% hydrogen peroxidase in methanol for 20 min. Sections were blocked against non-specific reactions

Table I. Tumor response in 16 patients treated with cisplatin-based neoadjuvant chemotherapy.

	No. of patients					
	CR	PR	SD	PD	Response rate (%)	P-value
Total	0	4	12	0	25	
No. of tumors						0.569
Solitary	0	3	5	0	37.5	
Multiple	0	1	7	0	12.5	
Tumor size (cm)						>0.999
≤3	0	2	6	0	25	
>3	0	2	6	0	25	
Stage						0.435
I	0	3	4	0	43	
II	0	1	6	0	14	
III	0	0	2	0	0	

CR, complete response; PR, partial response; SD, stable disease; PD, progressive disease.

with 10% normal rabbit serum, and were then incubated overnight at 4˚C with mouse anti-MRP2 monoclonal antibody (clone M2III-6; Monosan, Uden, The Netherlands; dilution at 1:20). Sections were then incubated with biotinylated rabbit anti-mouse immunoglobulin for 30 min followed by incubation with the streptavidin-peroxidase complex for 10 min. Diaminobenzidine was used as the chromogen, and the sections were counterstained with hematoxylin. Normal mouse immunoglobulin was substituted for the primary antibody as a negative control, whereas the immunoreactivity of adjacent non-neoplastic liver tissue was used as an internal positive control.

Pattern of MRP2 immunohistochemical expression in HCC. MRP2 expression was defined as the immunoreactivity of canalicular (apical) membranes of hepatocytes according to the description of Paulusma *et al* (4). Non-neoplastic hepatocytes showed weak to moderate intensity of MRP2 expression in the canalicular membrane. Immunoreactivity of MRP2 in tumor specimens was evaluated by comparison with adjacent non-neoplastic hepatocytes and classified into 3 categories: unchanged expression, when immunoreactivity of the tumor specimen was similar to that of non-neoplastic hepatocytes; loss-of-expression, characterized by totally negative immunoreactivity throughout the tumor specimen; and diffuse expression, characterized by strong positive immunoreactivity throughout the tumor specimen (Fig. 1). In the current study, overexpression of MRP2 was defined as diffuse expression, whereas non-overexpression was defined as unchanged or loss-of-expression.

Detection of MRP2 expression by Western blot analysis. Tissue samples were prepared for Western blotting by first snap-freezing and then stored at -80˚C until used for analysis. Tissue samples from 3 normal livers obtained at surgery for other conditions were processed for analysis as normal controls. Lysate from tissue samples were obtained by homogenization in the lysis buffer [20 mM Tris-buffered with 4-(2-hydroxyethyl)-1-piperazineethanesulfonic acid (HEPES) pH 8.0, 2 mM ethylenediaminetetraacetic acid (EDTA), 0.5 M sodium chloride, 0.5% sodium deoxycholate, 0.5% Triton X-100, 0.25 M sucrose, 50 mM 2-mercapto-ethanol, 250 μM phenylmethylsulfonyl fluoride and 1 μM pepstatin]. The lysate samples were kept on ice for 30 min, filtered through gauze and precleared by centrifugation at 15,000 rpm for 15 min at 4˚C. Following protein quantification using the Bradford assay (Bio-Rad Laboratories, Hercules, CA, USA), 50 μg aliquots of samples were resolved by sodium dodecyl sulfate-polyacrylamide gel electrophoresis and transferred to Immobilon membranes (Millipore, Bedford, MA, USA). Nonspecific sites binding sites on the membranes were blocked in 5% skim milk, whereupon filters were incubated with anti-MRP2 antibody (clone M2III-6; Monosan, Uden; dilution at 1:1000) and then the appropriate horseradish peroxidase-conjugated secondary antibodies. After the detection was performed using enhanced chemiluminescence reagent (GE Healthcare, Buckingham, UK), the blots were stripped, washed, and reprobed for ß-actin (Santa Cruz Biotechnology, Santa Cruz, CA, USA; dilution at 1:5000).

Statistical analysis. Medical records were obtained from all 49 patients. Categorical variables were compared by the Fisher exact test or the Pearson χ^2 test; continuous variables were compared by the Mann-Whitney U test. Correlation between 2 continuous variables was evaluated by the Spearman rank correlation. All statistical evaluations were performed using the SPSS 16.0J software package (SPSS Japan, Tokyo, Japan). All tests were two-sided and $P<0.05$ was considered statistically significant.

Results

Tumor response in 16 patients treated with cisplatin-based neoadjuvant chemotherapy. In 16 patients who received

Table II. Toxicity in 16 patients treated with cisplatin-based neoadjuvant chemotherapy.

Characteristics	No. of patients			
	Grade 1	Grade 2	Grade 3	Grade 4
Hematological toxicity				
Leukocytopenia	2	1	0	0
Anemia	0	1	0	0
Thrombocytopenia	2	2	0	0
Non-hematological toxicity				
Fever	2	0	0	0
Diarrhea	1	0	0	0
Decreased albumin level	2	7	0	0
Elevated total bilirubin level	4	1	0	0
Elevated AST level	2	8	2	0
Elevated ALT level	3	7	1	0
Elevated creatinine level	6	0	0	0

AST, aspartate aminotransferase; ALT, alanine aminotransferase.

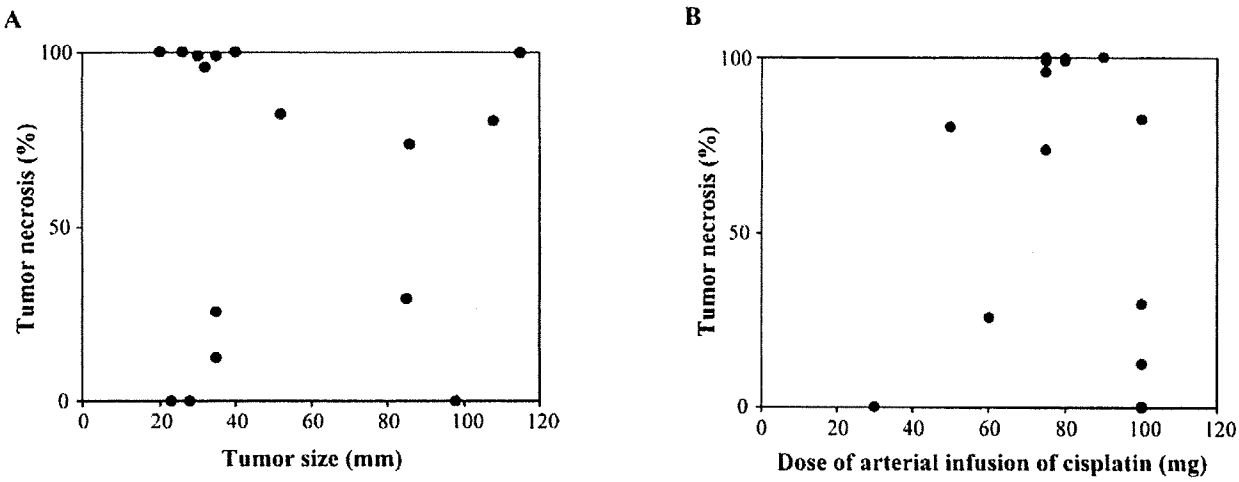

Figure 2. Correlation of tumor necrosis with tumor size and dose of cisplatin. (A) Tumor size prior to neoadjuvant chemotherapy does not correlate with tumor necrosis (correlation coefficient = -0.102; P=0.706). (B) The dose of hepatic arterial infusion of cisplatin has no correlation with tumor necrosis (correlation coefficient = -0.160; P=0.555).

cisplatin-based neoadjuvant chemotherapy, the median dose of cisplatin was 77.5 mg per body (range: 30-100 mg per body). The overall response rate of these patients was 25%; the therapeutic efficacy according to the RECIST guidelines was not associated with tested tumor-related factors (Table I).

Toxicity in 16 patients treated with cisplatin-based neoadjuvant chemotherapy. All 16 patients were assessed for toxicity and no toxic deaths occurred. The incidences of the main treatment-related toxicity according to the CTCAE version 4.0 are listed in Table II as the maximum grade seen per patient. No patients with grade 4 toxicities were identified. Three grade 3 non-hematological toxicities were observed. All hematological toxicities were grade 2.

Surgical resection. Hepatectomy procedures that were planned before neoadjuvant chemotherapy was administered were performed in all 16 patients who received the neoadjuvant chemotherapy. The interval between neoadjuvant chemotherapy and delayed surgery ranged from 30 to 114 days (median: 53 days). Operative procedures included major hepatectomy in 13 patients and minor hepatectomy in 36 patients. Complications during the postresection hospital stay occurred in 10 (20%) patients. Intra-abdominal sepsis (n=5) was the most common complication, followed by wound infection (n=4), biliary fistula (n=2), and pneumonia (n=1). The incidence of postoperative morbidity was 13% (2 of 16 patients) in patients treated with neoadjuvant chemotherapy compared with 24% (8 of 33 patients) in patients treated

Table III. Factors associated with MRP2 expression in 46 tumor specimens.

Variable	No. of patients		P-value
	Non-overexpression of MRP2	Overexpression of MRP2	
Age			0.568
≤70	13	12	
>70	9	12	
Sex			>0.999
Male	18	20	
Female	4	4	
Neoadjuvant chemotherapy			0.521
Absent	17	16	
Present	5	8	
Liver cirrhosis			0.763
Absent	7	9	
Present	15	15	
Tumor size (cm)			0.388
≤3	14	12	
>3	8	12	
Number of hepatic tumors			0.080
Solitary	16	11	
Multiple	6	13	
Edmondson-Steiner grade			0.507
I	4	4	
II	17	16	
III	1	4	
pT classification			0.625
pT1	13	11	
pT2	8	10	
pT3	1	3	
Vascular invasion			>0.999
Absent	18	20	
Present	4	4	

MRP2, multidrug resistance-associated protein 2; pT, pathologic T classification.

without neoadjuvant chemotherapy (P=0.464). There were no in-hospital deaths in the current series.

Tumor necrosis in resected specimens of 16 patients treated with cisplatin. The median percentage of histologically verified tumor necrosis was 81% (range: 0-100%). Complete tumor necrosis (no evidence of vivid tumor) was found in 3 patients [1 patient with PR (partial response) and 2 patients with SD (stable disease)], whereas no evidence of tumor necrosis was observed in 3 patients. Tumor size on CT images prior to neoadjuvant chemotherapy did not correlate with tumor necrosis of the resected specimens (P=0.706; Fig. 2A). The dose of hepatic arterial infusion of cisplatin did not correlate with tumor necrosis of the resected specimens (P=0.555; Fig. 2B). The median percentage of tumor necrosis was 99.4% (range: 73.6-100%) in 4 patients with PR, whereas it was 54.9% (range: 0-100%) in 12 patients with SD. There were no apparent differences in the percentage of tumor necrosis between 2 groups (PR vs. SD) according to the RECIST criteria by Mann-Whitney U test (P=0.138).

Immunohistochemical analysis of MRP2 expression. Three tissue samples with complete tumor necrosis were excluded from immunohistochemical analysis for MRP2. In the remaining 46 tissue samples, overexpression of MRP2 was detected in 24/46 (52%) of tumor specimens (Table III).

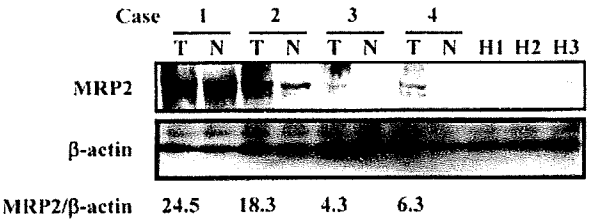

Figure 3. Western blot analysis for multidrug resistance-associated protein 2 (MRP2) levels. Based on immunohistochemical analysis, case 1 and 2 show overexpression of MRP2, whereas case 3 and 4 show non-overexpression of MRP2. The band intensities of tumor samples tested by Western blot analysis show a close correlation with the results of immunohistochemical analysis. MRP2 expression is faint in all healthy liver tissues. T; tumor, N; non-tumor, H1-3; healthy liver.

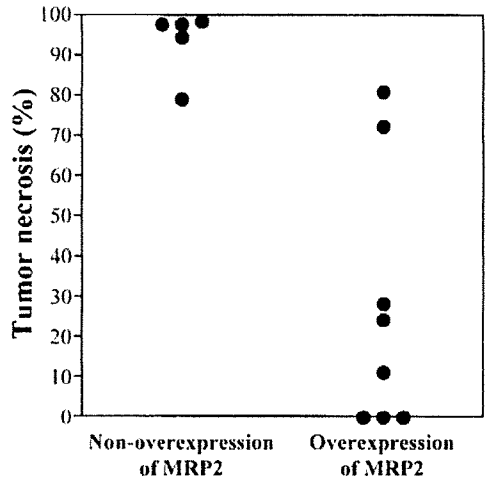

Figure 4. The extent of tumor necrosis in relation to the level of multidrug resistance-associated protein 2 (MRP2) expression. The percentage of tumor necrosis is significantly lower in tumor specimens with overexpression of MRP2 (median percentage of necrosis, 19%) than in tumor specimens with non-overexpression of MRP2 (median percentage of necrosis, 99%; P=0.003).

Loss-of-expression of MRP2 was found in 2/46 (4%) of tumor specimens; unchanged expression of MRP2 was observed in 20/46 (44%) of tumor specimens; and thus 22 tumor specimens were categorized as specimens with non-overexpression of MRP2.

Western blot analyses of MRP2 expression levels. To confirm the results of the immunohistochemical analysis for MRP2, we performed Western blot analysis on 5 randomly selected tumor samples with overexpression of MRP2, 5 tumor samples with non-overexpression of MRP2, and 3 tissue samples from healthy liver. Fig. 3 shows the representative results of Western blotting for MRP2 of selected tissue samples. MRP2 expression was faint in all healthy liver tissues tested by Western blot analysis, whereas the band intensities of tumor samples showed a close correlation with the results of immunohistochemical analysis.

Factors associated with MRP2 expression in 46 tumor specimens. Overexpression of MRP2 in tumor specimens was not associated with tested clinical-pathologic factors including neoadjuvant chemotherapy (Table III). Overexpression of MRP2 was detected in 16/33 (48%) of tumor specimens from patients treated without neoadjuvant chemotherapy, suggesting that nearly half of the patients with HCC have intrinsic overexpression of MRP2.

MRP2 expression and tumor necrosis in 13 tumor specimens containing vivid tumor from patients treated with cisplatin. We identified 8 tumor specimens with overexpression of MRP2 out of 13 tumor specimens containing vivid tumor from 16 patients treated with cisplatin-based neoadjuvant chemotherapy (Table III). Tumor specimens with overexpression of MRP2 showed a lower percentage of tumor necrosis (median percentage of necrosis, 19%) compared to tumor specimens with non-overexpression of MRP2 (median percentage of necrosis, 99%; P=0.003; Fig. 4).

Discussion

The activity of ABC transporters is one of the major causes of resistance to chemotherapy in patients with HCC (23). Of several identified ABC transporters, MRP2 is the principal cisplatin transporter (7-9). There is a paucity of clinical data regarding any relationship between MRP2 expression and tumor necrosis in patients treated with cisplatin-based neoadjuvant chemotherapy prior to hepatectomy for HCC. This prompted us to conduct the current study. This is the first study to demonstrate that MRP2 overexpression correlates with a lower percentage of tumor necrosis in tumors from patients treated with cisplatin-based neoadjuvant chemotherapy for HCC and thus expression of MRP2 determines the efficacy of cisplatin-based chemotherapy in patients with HCC.

Cisplatin is a widely used chemotherapeutic agent in the treatment of HCC (24). The fine-powder formulation of cisplatin has 3 times higher concentration compared to conventional formulations of cisplatin (25). Yoshikawa *et al* (25) reported that hepatic arterial infusion of a fine-powder formulation of cisplatin had a high therapeutic efficacy with a response rate of 33.8%. In the current study, we confirmed the results of Yoshikawa *et al* (25). Severe adverse effects (grade 3, liver dysfunction) were observed in 3 patients but they were manageable and transient. Planned hepatectomy procedures were performed in all 16 patients treated with neoadjuvant chemotherapy without any increase in post-operative complications. Thus, neoadjuvant chemotherapy with a fine-powder formulation of cisplatin is well tolerated and does not impair planned hepatectomy procedures.

We observed high tumor necrosis in the tumor specimens of patients who were treated with cisplatin-based neoadjuvant chemotherapy for HCC. In contrast, there were no apparent differences in the percentage of tumor necrosis between patients with PR and patients with SD according to RECIST criteria. In fact, complete tumor necrosis (no evidence of vivid tumor) was found in 2 patients with SD. Forner *et al* (26) have the questioned the reliability of RECIST criteria, which are based on the evaluation of unidimensional tumor measurements and disregard the extent of necrosis in solid liver tumors. Forner *et al* (26) recommended the evaluation

of tumor response based on measurements of the reduction in viable tumor burden as determined by dynamic imaging studies. Michaelis and Ratain (27) also suggested that RECIST criteria have limited value in the assessment of tumor response after chemotherapy because some anti-cancer agents have cytostatic, rather than cytotoxic properties, so that shrinkage of the tumor after cytostatic chemotherapy is not expected. Further investigation is required to develop effective criteria for the assessment of tumor response after chemotherapy.

MRP2 is a major transporter of conjugated bilirubin and bile salts into the bile canaliculi (5,6). In the current study, half of the tumor samples showed MRP2 overexpression, irrespective of administration of cisplatin (Table III). Since HCCs often produce bile, the intrinsic expression of MRP2 in HCC may partly explain their low sensitivity to some MRP2-dependent anti-cancer agents including cisplatin, doxorubicin, etoposide, and vincristine (7,28). Bonin *et al* documented that MRP2 mRNA expression level significantly increases in HCC compared to non-neoplastic liver tissue (14). In addition, Zollner *et al* using Western blot analysis found that MRP2 protein expression was elevated in all 4 HCC samples examined (13). In the current study, overexpression of MRP2 correlated with a lower percentage of tumor necrosis in patients treated with cisplatin-based neoadjuvant chemotherapy for HCC, whereas tumor size or dose of cisplatin did not. Collectively, these above findings suggest that expression of MRP2 determines the efficacy of cisplatin-based chemotherapy in patients with HCC.

Various classic compounds that inhibit MRP2 activity *in vitro* such as MK-571 or cyclosporin A have been proposed to be used to increase antitumor therapeutic effectiveness (29,30). The intrinsic toxicity of MRP2 inhibitors at doses necessary for their activity and their poor specificity are the major obstacles in applying them *in vivo* (8). In attempt to develop alternative, less toxic, and more efficient therapy, Meterna *et al* specifically inhibited MRP2 protein expression by 2 anti-MRP2 hammerhead ribozymes. This gene therapeutic approach may be applicable to overcome cisplatin resistance in tumor cells (8). Folmer *et al* demonstrated that tumors resulting from MRP2-overexpressing subcutaneously grown hepatoma cells, regressed in size upon antisense MRP2 expression in combination with vincristine (28). Wakamatsu *et al* reported that co-treatment with cisplatin and both glycyrrhizin and lamivudine inhibited the cisplatin efflux from Huh7 HCC cell line and concluded this was because glycyrrhizin is a competitive substrate for MRP2 (9). Therefore, it appears that inhibition of MRP2 may be an approach to develop an effective therapy to overcome cisplatin resistance in patients with HCC.

In interpreting the current study, we have considered the limitations of the analysis of a small number of patients and incomplete follow-up assessment of performed chemotherapeutic treatment using RECIST criteria. In fact, we believe that these limitations do not greatly influence the results of the study because the differences among groups were too marked to have resulted from these procedural biases.

In conclusion, overexpression of MRP2 correlates with a lower percentage of tumor necrosis in patients treated with cisplatin-based neoadjuvant chemotherapy for HCC, whereas either tumor size or dose of cisplatin does not. Expression of MRP2 determines the efficacy of cisplatin-based chemotherapy in patients with HCC.

References

1. Dean M, Rzhetsky A and Allikmets R: The human ATP-binding cassette (ABC) transporter superfamily. Genome Res 11: 1156-1166, 2001.
2. Mayer R, Kartenbeck J, Büchler M, Jedlitschky G, Leier I and Keppler D: Expression of the MRP gene-encoded conjugate export pump in liver and its selective absence from the canalicular membrane in transport-deficient mutant hepatocytes. J Cell Biol 131: 137-150, 1995.
3. Keppler D and Kartenbeck J: The canalicular conjugate export pump encoded by the *cmrp/cmoat* gene. In: Progress in Liver Diseases. Boyer JL and Ockner RK (eds). Saunders, Philadelphia, PA, pp55-67, 1996.
4. Paulusma CC, Kool M, Bosma PJ, Scheffer GL, ter Borg F, Scheper RJ, Tytgat GN, Borst P, Baas F and Oude Elferink RP: A mutation in the human canalicular multispecific organic anion transporter gene causes the Dubin-Johnson syndrome. Hepatology 25: 1539-1542, 1997.
5. Jedlitschky G, Leier I, Buchholz U, Hummel-Eisenbeiss J, Burchell B and Keppler D: ATP-dependent transport of bilirubin glucuronides by the multidrug resistance protein MRP1 and its hepatocyte canalicular isoform MRP2. Biochem J 327: 305-310, 1997.
6. Trauner M and Boyer JL: Bile salt transporters: molecular characterization, function, and regulation. Physiol Rev 83: 633-671, 2003.
7. Cui Y, König J, Buchholz JK, Spring H, Leier I and Keppler D: Drug resistance and ATP-dependent conjugate transport mediated by the apical multidrug resistance protein, MRP2, permanently expressed in human and canine cells. Mol Pharmacol 55: 929-937, 1999.
8. Materna V, Liedert B, Thomale J and Lage H: Protection of platinum-DNA adduct formation and reversal of cisplatin resistance by anti-MRP2 hammerhead ribozymes in human cancer cells. Int J Cancer 115: 393-402, 2005.
9. Wakamatsu T, Nakahashi Y, Hachimine D, Seki T and Okazaki K: The combination of glycyrrhizin and lamivudine can reverse the cisplatin resistance in hepatocellular carcinoma cells through inhibition of multidrug resistance-associated proteins. Int J Oncol 31: 1465-1472, 2007.
10. Koike K, Kawabe T, Tanaka T, Toh S, Uchiumi T, Wada M, Akiyama S, Ono M and Kuwano M: A canalicular multispecific organic anion transporter (cMOAT) antisense cDNA enhances drug sensitivity in human hepatic cancer cells. Cancer Res 57: 5475-5479, 1997.
11. Nies AT, König J, Pfannschmidt M, Klar E, Hofmann WJ and Keppler D: Expression of the multidrug resistance proteins MRP2 and MRP3 in human hepatocellular carcinoma. Int J Cancer 94: 492-499, 2001.
12. Vander Borght S, Libbrecht L, Blokzijl H, Faber KN, Moshage H, Aerts R, Van Steenbergen W, Jansen PL, Desmet VJ and Roskams TA: Diagnostic and pathogenetic implications of the expression of hepatic transporters in focal lesions occurring in normal liver. J Pathol 207: 471-482, 2005.
13. Zollner G, Wagner M, Fickert P, Silbert D, Fuchsbichler A, Zatloukal K, Denk H and Trauner M: Hepatobiliary transporter expression in human hepatocellular carcinoma. Liver Int 25: 367-379, 2005.
14. Bonin S, Pascolo L, Crocé LS, Stanta G and Tiribelli C: Gene expression of ABC proteins in hepatocellular carcinoma, perineoplastic tissue, and liver diseases. Mol Med 8: 318-325, 2002.
15. Cruz PV, Wakai T, Shirai Y, Yokoyama N and Hatakeyama K: Loss of carcinoembryonic antigen-related cell adhesion molecule 1 expression is an adverse prognostic factor in hepatocellular carcinoma. Cancer 104: 354-360, 2005.
16. Wakai T, Shirai Y, Sakata J, Kaneko K, Cruz PV, Akazawa K and Hatakeyama K: Anatomic resection independently improves long-term survival in patients with T1-T2 hepatocellular carcinoma. Ann Surg Oncol 14: 1356-1365, 2007.
17. Korita PV, Wakai T, Shirai Y, Matsuda Y, Sakata J, Cui X, Ajioka Y and Hatakeyama K: Overexpression of osteopontin independently correlates with vascular invasion and poor prognosis in patients with hepatocellular carcinoma. Hum Pathol 39: 1777-1783, 2008.

18. Therasse P, Arbuck SG, Eisenhauer EA, Wanders J, Kaplan RS, Rubinstein L, Verweij J, Van Glabbeke M, van Oosterom AT, Christian MC and Gwyther SG: New guidelines to evaluate the response to treatment in solid tumors. European Organization for Research and Treatment of Cancer, National Cancer Institute of the United States, National Cancer Institute of Canada. J Natl Cancer Inst 92: 205-216, 2000.
19. Cancer Therapy Evaluation Program. Common Terminology Criteria for Adverse Events. Version 4.0. National Cancer Institute. Available from URL: http://ctep.cancer.gov/protocolDevelopment/electronic_applications/ctc.htm.
20. Sobin LH and Wittekind C: TNM Classification of Malignant Tumours. 6th edition. UICC, Wiley-Liss, New York, pp81-83, 2002.
21. Taylor M, Forster J, Langer B, Taylor BR, Greig PD and Mahut C: A study of prognostic factors for hepatic resection for colorectal metastases. Am J Surg 73: 467-471, 1997.
22. Edmondson HA and Steiner PE: Primary carcinoma of the liver: a study of 100 cases among 48,900 necropsies. Cancer 7: 462-503, 1954.
23. Le Vee M, Jigorel E, Glaise D, Gripon P, Guguen-Guillouzo C and Fardel O: Functional expression of sinusoidal and canalicular hepatic drug transporters in the differentiated human hepatoma HepaRG cell line. Eur J Pharm Sci 28: 109-117, 2006.
24. Carr BI: Hepatocellular carcinoma: current management and future trends. Gastroenterology 127 (Suppl 1): S218-S224, 2004.
25. Yoshikawa M, Ono N, Yodono H, Ichida T and Nakamura H: Phase II study of hepatic arterial infusion of a fine-powder formulation of cisplatin for advanced hepatocellular carcinoma. Hepatol Res 38: 474-483, 2008.
26. Forner A, Ayuso C, Varela M, Rimola J, Hessheimer AJ, de Lope CR, Reig M, Bianchi L, Llovet JM and Bruix J: Evaluation of tumor response after locoregional therapies in hepatocellular carcinoma: are response evaluation criteria in solid tumors reliable? Cancer 115: 616-623, 2009.
27. Michaelis LC and Ratain MJ: Measuring response in a post-RECIST world: from black and white to shades of grey. Nat Rev Cancer 6: 409-414, 2006.
28. Folmer Y, Schneider M, Blum HE and Hafkemeyer P: Reversal of drug resistance of hepatocellular carcinoma cells by adenoviral delivery of anti-ABCC2 antisense constructs. Cancer Gene Ther 14: 875-884, 2007.
29. Leier I, Jedlitschky G, Buchholz U, Cole SP, Deeley RG and Keppler D: The MRP gene encodes an ATP-dependent export pump for leukotriene C4 and structurally related conjugates. J Biol Chem 269: 27807-27810, 1994.
30. Chen ZS, Kawabe T, Ono M, Aoki S, Sumizawa T, Furukawa T, Uchiumi T, Wada M, Kuwano M and Akiyama SI: Effect of multidrug resistance-reversing agents on transporting activity of human canalicular multispecific organic anion transporter. Mol Pharmacol 56: 1219-1228, 1999.

Computer-aided Diagnosis of Focal Liver Lesions by Use of Physicians' Subjective Classification of Echogenic Patterns in Baseline and Contrast-enhanced Ultrasonography[1]

Katsutoshi Sugimoto, MD, Junji Shiraishi, PhD, Fuminori Moriyasu, MD, Kunio Doi, PhD

Rational and Objectives. To develop a computer-aided diagnostic (CAD) scheme for classifying focal liver lesions (FLLs) by use of physicians' subjective classification of echogenic patterns of FLLs on baseline and contrast-enhanced ultrasonography (US).

Materials and Methods. A total of 137 hepatic lesions in 137 patients were evaluated with B-mode and NC100100 (Sonazoid)-enhanced pulse-inversion US; lesions included 74 hepatocellular carcinomas (HCCs) (23: well-differentiated, 36: moderately differentiated, 15: poorly differentiated HCCs), 33 liver metastases, and 30 liver hemangiomas. Three physicians evaluated single images at B-mode and arterial phases with a cine mode. Physicians were asked to classify each lesion into one of eight B-mode and one of eight enhancement patterns, but did not make a diagnosis. To classify five types of FLLs, we employed a decision tree model with four decision nodes and four artificial neural networks (ANNs). The results of the physicians' pattern classifications were used successively for four different ANNs in making decisions at each of the decision nodes in the decision tree model.

Results. The classification accuracies for the 137 FLLs were 84.8% for metastasis, 93.3% for hemangioma, and 98.6% for all HCCs. In addition, the classification accuracies for histological differentiation types of HCCs were 65.2% for well-differentiated HCC, 41.7% for moderately differentiated HCC, and 80.0% for poorly differentiated HCC.

Conclusions. This CAD scheme has the potential to improve the diagnostic accuracy of liver lesions. However, the accuracy in the histologic differential diagnosis of HCC based on baseline and contrast-enhanced US is still limited.

Key Words. Contrast-enhanced sonography; computer-aided diagnosis; focal liver lesion; Sonazoid.

In the diagnosis of focal liver lesions (FLLs) including hepatocellular carcinoma (HCC), liver metastases, hemangioma, and focal nodular hyperplasia (FNH), contrast-enhanced computed tomography (CT) (1) and magnetic resonance imaging (MRI) (2–4) have been employed more commonly than ultrasonography (US). However, the ultrasonographic equipment is less expensive and can be installed easily compared with CT and MRI. Therefore, US may become more popular in the future, especially in the developing countries. In addition, contrast-enhanced US (CEUS) with pulse-inversion (5) (phase-inversion) imaging techniques has been applied for improvement of the diagnostic accuracy of FLLs. Recently, second-generation ultrasonographic contrast agents, such as DMP 115 (Definity; Lantheus Inc., MA) in Canada and BR 1 (SonoVue; Bracco, Milan, Italy) in Europe and China, have been applied in clinical practice. The agent NC100100 (Sonazoid; GE Healthcare, Oslo, Norway) has become clinically available since January 2007, in Japan ahead of other countries. Although the second-generation ultrasonographic contrast agents have not yet been applied in clinical practice

Acad Radiol 2009; 16:401–411

[1] From the Kurt Rossmann Laboratories for Radiologic Imaging Research, Department of Radiology, The University of Chicago, 5841 S. Maryland Ave., MC 2026, Chicago, IL 60637 (K.S., J.S., K.D.); Department of Gastroenterology and Hepatology, Tokyo Medical University, Tokyo, Japan (K.S., F.M.). Received August 22, 2008; accepted September 24, 2008. **Address correspondence to:** K.S. e-mail: sugimoto@comcast.net

doi:10.1016/j.acra.2008.09.018

for the diagnosis of FLLs in United States, CEUS with these agents are being widely used worldwide.

The problem with US, however, is a disparity in the diagnostic accuracy among institutions. Generally, US strongly depends on subjective aspect of the sonologist, compared to CT and MRI (6). Although this problem has not been so serious in so-called "high-volume centers," where US is used routinely for the diagnosis of FLLs, the diagnostic accuracy in an institution where US is performed infrequently can be poorer than that in a "high-volume center." For reducing this disparity as much as possible, the development of a computer-aided diagnosis (CAD) scheme for the classification of FLLs on CEUS has been attempted (7).

The concept and methodology of CAD to assist physicians in detecting abnormal lesions and improving the classification accuracy of the differential diagnosis have been developed and studied in various radiologic imaging fields (8,9). CAD may be defined as a diagnosis made by physicians who take into account the results of automated computer analysis of medical images. The computer output may be used as a "second opinion" for improving physicians' decision-making and avoiding oversights. In this study, we developed and assessed a CAD scheme for classifying FLLs into liver metastasis, hemangioma, and three histologic differentiation types of HCC using physicians' subjective classifications of echogenic patterns of FLLs on baseline US and CEUS.

MATERIALS AND METHODS

Patient Population

The study was approved by the research ethics board of the Tokyo Medical University, Tokyo, Japan; written informed consent was obtained from each patient for the use of ultrasonographic data for research purposes. Between January 2007 and October 2007, we used conventional US to examine 150 consecutive patients who had hepatic tumors. These patients were recruited at the Tokyo Medical University Hospital. In this study, we excluded patients who were critically ill, were hypersensitive to drugs, and/or had lesions that had been characterized by baseline US (ie, obvious cysts and focal fatty sparings). This study was exempted from the review of the institutional review board at the University of Chicago, because no patient information at this institution was used in this study.

The final diagnosis of the lesions indicated that there were 74 patients with HCC (23 well-differentiated, 36 moderately differentiated, 15 poorly differentiated HCCs), 33 patients with liver metastases (18 colon carcinomas, five gastric carcinomas, two pancreatic carcinomas, two rectal carcinomas, two ovarian carcinomas, two lung carcinomas, one bladder carcinoma, one breast carcinoma), 30 patients with hemangioma, five patients with FNH, three with focal fatty sparings, two with peripheral cholangiocarcinomas, two with dysplastic nodules, and one with an epithelioid hemangioendothelioma. All HCCs, liver metastases, FNH, focal fatty sparings, peripheral cholangiocarcinomas, dysplastic nodules, and epithelioid hemangioendothelioma were diagnosed using histologic examination after surgical resection (10 lesions), or by US-guided biopsy (110 lesions). The degree of cellular differentiation (defined as well-, moderately, or poorly differentiated HCC) was determined according to the International Working Party classification (10). The diagnosis of hemangioma was confirmed using contrast-enhanced CT and/or MRI and by the absence of any changes on follow-up imaging after more than 4 months.

For this study, we excluded five patients with FNH, three patients with focal fatty sparings, two patients with dysplastic nodules, two patients with peripheral cholangiocarcinomas, and one patient with epithelioid hemangioendothelioma because the number of the lesions was small. The 137 remaining patients were enrolled in this study. Of these, 107 patients had solitary focal lesions and 30 had multiple focal lesions. For the patients who had more than one focal lesion, the largest and most conspicuous lesion was evaluated; therefore, 137 hepatic lesions were studied.

With regard to the age distribution for each tumor type, there were no significant differences in the mean age between men and women among the patients with HCC (men, 66.1 ± 10.4 years; women, 74.5 ± 8.1 years), patients with metastases (men, 69.4 ± 9.5 years; women, 66.6 ± 10.3 years), and patients with hemangiomas (men, 54.4 ± 12.5 years; women, 53.0 ± 15.2 years). The size of each of the hepatic tumors was measured during baseline US by a physician (K.S.) who had 8 years of experience in liver ultrasonographic imaging and 5 years of experience in CEUS of the liver. The mean maximum tumor diameter was 25 ± 19 mm among HCCs (18 ± 8 mm among well-differentiated HCCs, 22 ± 17 mm among moderately differentiated HCCs, 41 ± 23 mm among poorly differentiated HCCs), 35 ± 15 mm among metastases, and 28 ± 17 mm among hemangiomas. All ultrasonographic scans were performed by the same physician, who was aware of the patients' clinical history and who was blinded to the biopsy results and all imaging findings except those of US.

Ultrasonographic Technique

The ultrasonographic equipment used was a SSA-790A (Aplio XG; Toshiba Medical Systems Corp., Otawara, Japan). First, each lesion was scanned at baseline US. Each focal liver lesion was identified on baseline US and assigned a liver segment location according to Couinaud's (11) and Bismuth's (12) classification systems.

The contrast agent used in this study, NC100100, consists of perflubutane microbubbles surrounded by phospholipids.

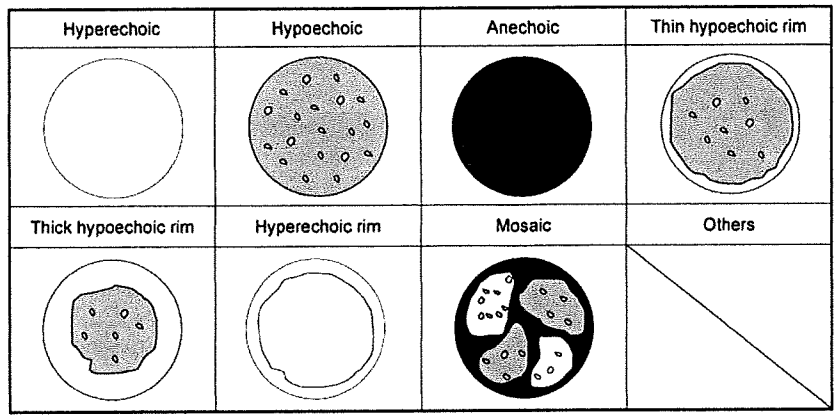

a.

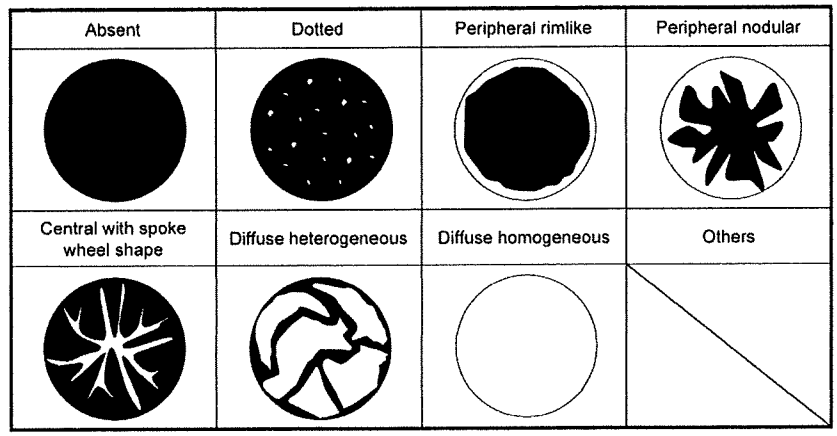

b.

Figure 1. **(a)** Illustration of morphologic patterns of hepatic tumors in the B-mode ultrasonography. **(b)** Illustration of enhancement patterns of hepatic tumors in the arterial phase.

The average diameter of the microbubbles is 2–3 μm. The contrast agent was injected as a 0.5 mL bolus into an antecubital vein with a 21-gauge peripheral intravenous cannula, followed by a 10 mL saline flush. The ultrasonographic equipment used was a SSA-790A with a 3.75-MHz convex transducer (PVT-375BT). The imaging mode was wideband harmonic imaging (commercially called Pulse subtraction) with transmission and reception frequencies of 3.75 and 7.5 MHz, respectively. When a suspected lesion was identified, a dynamic CEUS was performed with the focus depth beyond the region of interest, at a frame rate of 15 frames/s and a dynamic range of 45 dB. The mechanical index values were between 0.2 and 0.3, so that the microbubbles could be preserved throughout their half-life in microvessels and real-time exploration of the liver vasculature could be preserved. The region of interest was observed continuously for about 3 minutes from the time of injection (observation of the vascular phase). After 3 minutes, we froze the scan. Approximately 10 minutes after injection of the contrast agent to allow pooling of the agent in the hepatic parenchyma, we observed the tumors for enhancement using a sweep scan (observation of the delayed phase). Digital cine clips were stored during baseline US scanning and during the arterial phase (ie, 10–40 seconds from the beginning of the injection of the contrast agent bolus), during the portal phase (ie, 50–90 seconds from the beginning of the injection), the late phase (ie, 100–180 seconds from the beginning of the injection), and the delayed phase (ie, 10 minutes from the beginning of the injection).

Observer study for Obtaining Subjective Classifications of Echogenic Patterns

Digital cine clips stored on a digital hard disk were reviewed by three readers independently on a PC (VGN-S94PS; SONY, Tokyo, Japan). The readers were physicians trained in the use and interpretation of contrast agents in the liver. They were not involved in the ultrasonographic scanning and were

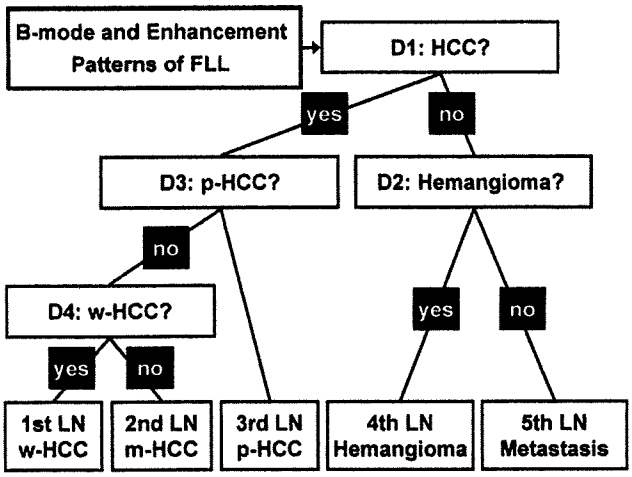

Figure 2. Illustration of the decision tree model used in this study. Four decision nodes in which alternative choice was determined by all five FLLs, leading to a final diagnostic decision for five liver lesions. D, decision node; FLL, focal liver lesion; HCC, hepatocellular carcinoma; LN, leaf node; m-HCC, moderately differentiated HCC; p-HCC, poorly differentiated HCC; w-HCC, well-differentiated HCC.

blinded to the identification, clinical histories, biopsy results, and other imaging findings of the patients. A clinical fellow in body imaging who was trained in contrast US, who neither scanned the patients nor was a reader, selected representative images and digital cine clips to show the baseline appearance as well as the arterial phase enhancement of the lesion. Cine clips were presented in a random order, and any identifying information was masked. In this study, we used only baseline and arterial-phase images.

From the baseline ultrasonographic features of a single mass in only one image, the reviewers were requested to classify the echogenic patterns of the mass into one of the following eight patterns: 1) hyperechoic; 2) hypoechoic; 3) anechoic with posterior echo enhancement; 4) thin hypoechoic rim; 5) thick irregular hypoechoic rim (bull's eye); 6) echogenic rim; 7) mosaic; and 8) others (Fig 1a). These patterns were proposed by Itai et al (13) for describing the characteristics of FLLs on baseline US.

After the ratings of echogenic patters of FLLs on the baseline US, the readers were asked to classify the contrast enhancement pattern of FLLs into one of the following eight patterns: 1) absent; 2) dotted; 3) peripheral rimlike; 4) peripheral nodular; 5) central with spoke wheel shape; 6) diffuse homogeneous; 7) diffuse heterogeneous; and 8) others (Fig 1b), which were proposed by Quaia et al (14). The readers were not asked to provide a diagnosis of an FLL in this observer study.

For employing these subjective ratings obtained by three readers classifying 137 FLLs using a computerized scheme, we created a matrix of 137 FLLs and 16 patterns, which indicated the total number of readers who rated the lesions for each pattern.

Computer-aided Diagnostic Scheme for the Classification of FLLs

To classify five types of FLLs (eg, well-differentiated, moderately differentiated, poorly differentiated HCC, liver metastasis, and liver hemangioma) in this CAD scheme, we employed four artificial neural networks (ANNs) as shown in Figure 2. ANNs are mathematical models based on biologic neural networks. These consist of an interconnected group of artificial neurons and processes information using a connectionist approach to computation. The order of the four decisions (labeled D1–D4) at each ANN was determined based on the diagnostic difficulties based on the physicians' knowledge. The four decisions used in this study were as follows:

D1: Is this lesion a HCC (yes) or other (no)?
D2: Is this lesion a hemangioma (yes) or metastasis (no)?
D3: Is this lesion a poorly differentiated HCC (yes) or other HCC (no)?
D4: Is this lesion a well-differentiated HCC (yes) or a moderately differentiated HCC (no)?

All decisions were determined using each of the ANNs in terms of a two-alternative choice method. In all of the four ANNs, we used 14 input units corresponding to each of seven patterns of subjective classification data in the matrix as described previously, and one image feature of the effective diameter of an FLL. We did not use one of the subjective classifications (others), because we assumed that these uncertain data might have a detrimental effect on the training of the ANNs. The effective diameter was calculated from a contour of an FLL, which was provided by a physician (K.S.).

We used the same parameter settings for the four ANNs, such as one hidden layer, eight hidden units, one output unit, 0.05 for the learning rate, and 0.30 for the slope of the sigmoid function except for the numbers of iterations for learning (15,16). The four ANNs were trained and tested independently by use of a leave-one-lesion-out test method. The range of iteration numbers between 200 and 600 with intervals of 100 were examined independently by monitoring of the accuracy in distinguishing between two groups for each ANN. Finally, we determined the number of iterations, such as 200 for D1 and D2, 400 for D3, and 600 for D4.

The correct classification of the CAD scheme for the five types of FLLs was determined when the final outcome from the four ANNs agreed with the "gold standard." The classification accuracies for each type of FLL and also for all 137 FLLs were determined with percentages of correctly classified cases among the total number of cases.

Table 1
The Total Number of Lesions Rated by Three Readers for Subjective Classification of Eight Ultrasonographic Patterns of B-mode Imaging

		Classification by Three Readers															
Lesion	Number of Lesions	Hyperechoic		Hypoechoic		Anechoic		Thin Hypoechoic Rim		Thick Hypoechoic Rim		Hyperechoic Rim		Mosaic		Others	
HCC	74	18	(8%)	92	(41%)	0	(0%)	50	(23%)	4	(2%)	3	(1%)	44	(20%)	11	(5%)
w-HCC	23	2	(3%)	42	(61%)	0	(0%)	9	(13%)	1	(1%)	1	(1%)	11	(16%)	3	(4%)
m-HCC	36	11	(10%)	42	(39%)	0	(0%)	29	(27%)	2	(2%)	1	(1%)	17	(16%)	6	(6%)
p-HCC	15	5	(11%)	8	(18%)	0	(0%)	12	(27%)	1	(2%)	1	(2%)	16	(36%)	2	(4%)
Metastasis	33	16	(14%)	24	(24%)	2	(2%)	5	(5%)	42	(42%)	0	(0%)	3	(3%)	7	(7%)
Hemangioma	30	37	(41%)	27	(30%)	0	(0%)	2	(2%)	0	(0%)	22	(24%)	2	(2%)	0	(0%)

Note. Numbers in parentheses are the percentage for the mean number of readers who rated the lesions for each pattern.
m-HCC, moderately differentiated hepatocellular carcinoma; p-HCC, poorly differentiated hepatocellular carcinoma; w-HCC, well-differentiated hepatocellular carcinoma.

Table 2
The Total Number of Lesions Rated by Three Readers for Subjective Classification of Eight Ultrasonographic Patterns of Contrast Harmonic Imaging

		Classification by Three Readers															
Lesion	Number of Lesions	Absent		Dotted		Peripheral Rimlike		Peripheral Nodular		Central with Spoke Wheel Shape		Diffuse Homogeneous		Diffuse Heterogeneous		Others	
HCC	74	0	(0%)	0	(0%)	2	(1%)	19	(9%)	0	(0%)	104	(47%)	97	(44%)	0	(0%)
w-HCC	23	0	(0%)	0	(0%)	0	(0%)	2	(3%)	0	(0%)	34	(49%)	33	(48%)	0	(0%)
m-HCC	36	0	(0%)	0	(0%)	1	(1%)	6	(6%)	0	(0%)	69	(64%)	32	(30%)	0	(0%)
p-HCC	15	0	(0%)	0	(0%)	1	(2%)	11	(24%)	0	(0%)	1	(2%)	32	(71%)	0	(0%)
Metastasis	33	0	(0%)	0	(0%)	28	(28%)	40	(40%)	2	(2%)	1	(1%)	28	(28%)	0	(0%)
Hemangioma	30	0	(0%)	0	(0%)	45	(50%)	43	(48%)	0	(0%)	2	(2%)	0	(0%)	0	(0%)

Note. Numbers in parentheses are the percentage for the mean number of readers who rated the lesions for each pattern.
m-HCC, moderately differentiated hepatocellular carcinoma; p-HCC, poorly differentiated hepatocellular carcinoma; w-HCC, well-differentiated hepatocellular carcinoma.

RESULTS

Table 1 shows the distribution of morphologic patterns of the hepatic tumors as rated by three readers on baseline US. The following are the approximate average numbers of the type of lesions rated by the three readers. The results indicated that 30 (41%) of the 74 HCCs were visualized as having a hypoechoic pattern; 14 (42%) of the 33 liver metastases were visualized as having a thick, irregular hypoechoic rim pattern; 12 (41%) of the 30 hemangiomas had a hyperechoic pattern; 14 (61%) of the 23 well-differentiated HCCs; 14 (39%) of the 36 moderately differentiated HCCs were classified as having a hypoechoic pattern; and 5 (36%) of 15 the poorly differentiated HCCs were classified as having a mosaic pattern.

Table 2 shows the distribution of enhancement patterns of the hepatic tumors as rated by the three readers on CEUS. In the arterial phase, 67 (91%) of the 74 HCCs exhibited a homogeneous or heterogeneous pattern of enhancement; 35 (47%) exhibited a homogeneous pattern and 33 (44%) exhibited a heterogeneous pattern; 13 (40%) of the 33 liver metastases exhibited a peripheral nodular pattern of enhancement; 15 (50%) of the 30 liver hemangiomas exhibited a peripheral rimlike pattern of enhancement; 22 (97%) of the 23 well-differentiated HCCs exhibited a homogeneous or heterogeneous pattern of enhancement; 12 (49%) exhibited a homogeneous pattern and 11 (48%) exhibited a heterogeneous pattern; 23 (64%) of the 36 moderately differentiated HCCs exhibited a homogeneous pattern of enhancement; and 11 (71%) of the 15 poorly differentiated HCCs exhibited a heterogeneous pattern of enhancement.

The computer performance in terms of the number of FLLs correctly classified and the classification accuracies (%) in each of the four ANNs were 133 of 137 (97.1%) for

Table 3
Performance of CAD Scheme for Classification in Five Categories Using Physicians' Subjective Pattern Classification

		Classification with CAD									
		HCC									
Lesion	Number of Lesions	w-HCC		m-HCC		p-HCC		Metastasis		Hemangioma	
HCC	74										
w-HCC	23	15	(65.2%)	4	(17.4%)	4	(17.4%)	0	(0.0%)	0	(0.0%)
m-HCC	36	16	(44.4%)	15	(41.7%)	5	(13.9%)	0	(0.0%	1	(2.7%)
p-HCC	15	1	(6.7%)	1	(6.7%)	12	(80.0%)	1	(6.7%)	0	(0.0%)
Metastasis	33	1	(3.0%)	0	(0.0%)	1	(3.0%)	28	(84.8%)	3	(9.1%)
Hemangioma	30	0	(0.0%)	0	(0.0%)	1	(3.3%)	1	(3.3%)	28	(93.3%)

CAD, computed-aided diagnosis; m-HCC, moderately differentiated hepatocellular carcinoma; p-HCC, poorly differentiated hepatocellular carcinoma; w-HCC, well-differentiated hepatocellular carcinoma.
Overall diagnostic accuracy: 98/137 (71.5 %).
CAD performance was evaluated by a leave-one-case-out method.

D1, 56 of 63 (88.9%) for D2, 62 of 74 (83.9%) for D3, and 20 of 59 (66.1%) for D4. Table 3 shows the performance of the computerized scheme for the classification of the five types of FLLs. The classification accuracies for the 137 FLLs were 84.8% for metastasis, 93.3% for hemangioma, 65.2% for well-differentiated HCC, 41.7% for moderately differentiated HCC, and 80.0% for poorly differentiated HCC. When the classification was conducted only for three types of FLLs (HCCs, metastasis, and hemangioma), the classification accuracy for all HCCs was 98.6%, as shown in Table 4. The average classification accuracies for three and five types of FLLs were 94.2% and 71.5%, respectively.

Figures 3 to 7 show examples of baseline and contrast-enhanced ultrasonographic images for each of the five types of FLLs that were classified correctly by the CAD. The results in Table 3 indicated that eight FLLs were incorrectly classified by the CAD into three types of FLLs, which consisted of one HCC, five metastases, and two hemangiomas. The CAD incorrectly classified one HCC as a metastasis, five metastases as two HCCs and three hemangiomas, and two hemangiomas as one HCC and one metastasis. Therefore, the classification accuracies for malignant (HCCs and metastases) and for benign (hemangiomas) lesions were 94.4% and 93.3%, respectively.

DISCUSSION

The characterization of FLLs using state-of-the-art US includes a gray-scale morphologic evaluation coupled with vascular information derived from color or power Doppler US (17). The comparison of conventional US with contrast-enhanced CT and MRIs for characterization of liver masses, however, shows that US is generally inferior at this task (18–21).

Table 4
Performance of CAD Scheme for Classification in Three Categories Using Physicians' Subjective Pattern Classification

		Classification with CAD			
Lesion	Number of Lesions	HCC		Metastasis	Hemangioma
HCC	74	73	(98.6%)	1 (1.4%)	0 (0.0%)
Metastasis	33	2	(6.1%)	28 (84.8%)	3 (9.1%)
Hemangioma	30	1	(3.3%)	1 (3.3%)	28 (93.3%)

CAD, computed-aided diagnosis; HCC, hepatocellular carcinoma.
Overall diagnostic accuracy: 129/137 (94.2 %).
CAD performance was evaluated by a leave-one-case out method.

The more recent introduction of second-generation ultrasonographic contrast agents such as DMP 115, BR 1, and NC100100, together with newer imaging techniques, has provided much better imaging capabilities. These agents may be imaged at a low mechanical index, thus preserving the microbubbles and allowing real-time and continuous imaging of both a lesion and its vessels. Among recent reports evaluating these second-generation ultrasonographic contrast agents, Quaia et al (14) demonstrated that the overall diagnostic accuracy in the discrimination between benign and malignant tumors of the liver by readers 1 and 2 was 49% and 51% before the use of a contrast agent and increased to 85% and 88% after the use of the contrast agent, respectively. In addition, Wilson et al (22) reported that the overall diagnostic accuracy with the use of their algorithm was 86% (25 of 29) in HCC, 73% (11 of 15) in non-HCC malignancy, 92% (24 of 26) in hemangioma, and 95% (19 of 20) in FNH. Their algorithm is designed primarily to classify the lesions according to the presence or absence of sustained enhancement

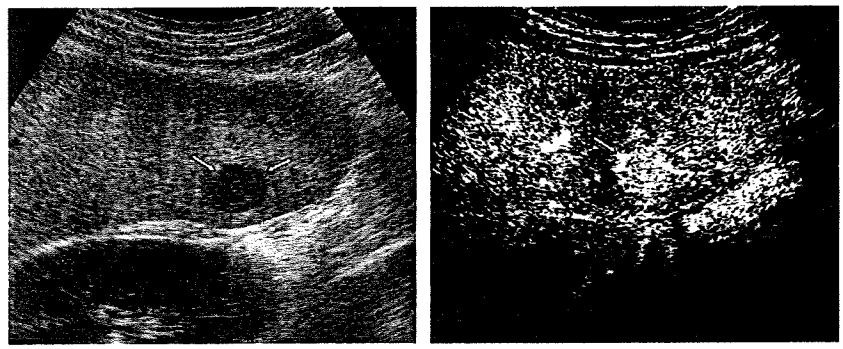

a. b.

Figure 3. A 28-year-old man with alcoholic cirrhosis and hepatocellular carcinoma *(arrows)*. **(a)** Sagittal B-mode ultrasound shows hypoechoic mass *(arrows)* in right lobe of liver. **(b)** In arterial phase, lesion *(arrows)* shows diffuse homogeneous and slightly hypervascularity relative to liver parenchyma. Percutaneous biopsy revealed well-differentiated hepatocellular carcinoma.

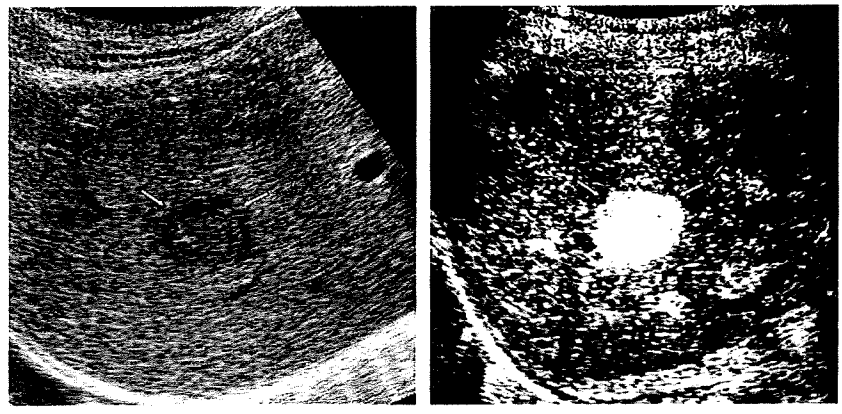

a. b.

Figure 4. A 73-year-old woman with hepatitis C cirrhosis and hepatocellular carcinoma *(arrows)*. **(a)** Oblique subcostal B-mode ultrasound shows mass *(arrows)* with thin hypoechoic rim in right lobe of liver. **(b)** In arterial phase, the lesion *(arrows)* shows diffuse homogeneous and fairly hypervascularity relative to liver parenchyma. Percutaneous biopsy revealed moderately differentiated hepatocellular carcinoma.

in the extended portal phase. According to their classification, 48 (92%) of 52 benign lesions showed positive or sustained enhancement, and 41 (93%) of 44 malignancies showed negative enhancement or washout in the extended portal phase.

In our present study, to establish CAD for the diagnosis of FLLs, we used morphologic features as image features of hepatic tumors on baseline US and the contrast enhancement pattern in the arterial phase of contrast-enhanced US. However, we did not use findings from the portal, late, or delayed phase (ie, the presence or absence of washout) as image features of our CAD.

The diagnosis of hepatic tumors by baseline US is generally considered nonspecific. In fact, Itai et al (13) reported that the average diagnostic accuracy of hepatic tumors by baseline US was 68% in HCC, 77% in metastatic liver tumors, and 77% in hemangiomas. However, mosaic and hypoechoic patterns are findings that are relatively specific for HCC, and the sensitivity of mosaic and hypoechoic patterns is reported to be 91% and 92%, respectively. Therefore, we used baseline ultrasonographic images as the basis to establish CAD for the diagnosis of FLLs.

According to Jang et al (23), the dysmorphic vessels of HCC are distinctly different from the central stellate vessels demonstrated in FNH or peripheral nodular enhancement of hemangioma in the arterial phase. Therefore, the authors reported that a careful analysis of the vascular morphology during the wash-in of contrast material often contributes to

a. b.

Figure 5. A 75-year-old man with hepatitis C cirrhosis and hepatocellular carcinoma *(arrows)*. **(a)** Oblique subcostal left-lobe B-mode ultrasound shows mosaic mass *(arrows)*. **(b)** In the arterial phase, lesion *(arrows)* shows diffuse heterogeneous and slightly hypovascularity relative to liver parenchyma. Percutaneous biopsy revealed poorly differentiated hepatocellular carcinoma.

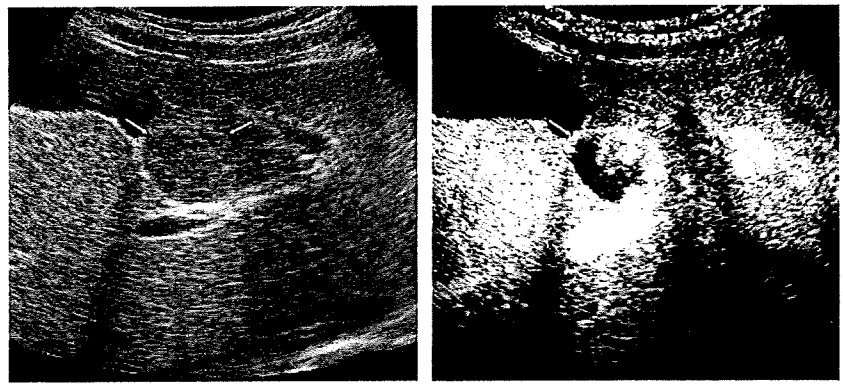

a. b.

Figure 6. A 38-year-old woman with liver hemangioma *(arrows)*. **(a)** Oblique subcostal B-mode ultrasound shows mass with hyperechoic rim *(arrows)*. **(b)** In the arterial phase, the image shows peripheral puddles of contrast that were enhanced more than the adjacent liver parenchyma.

the diagnosis of HCC and its differentiation from other benign tumors. Thus, the arterial phase is assumed to be one of the most important phases for the differential diagnosis of hepatic tumors. However, Wilson et al (22) and Quaia et al (14) reported that the presence or absence of washout in the portal phase and late phase (referred to as extended portal phase by Wilson et al) would be considered useful in the differential diagnosis of hepatic tumors, especially between benign and malignant tumors. The reason for our use of image findings only in the arterial phase as image features is as follows. In our present study, we used the reviewers' subjective data for CAD input data, although our future goal is to recognize the ultrasonographic image data automatically as input data to the CAD system. However, it is difficult to recognize automatically all of the data in a dynamic-imaging series for input data because of the problem of timing of patients' breath holding. We therefore used images only in the arterial phase, which is affected less by breathing.

According to the results of the pattern classification of baseline US, HCCs were most frequently classified into a hypoechoic pattern (41%), followed by a thin hypoechoic rim pattern (23%) and a mosaic pattern (20%). Makuuchi et al (24) described the mosaic pattern as architecture specific for HCC; this finding included 81% of HCCs ranging from 2 to 5 cm in diameter. However, the frequency of this finding obviously decreased as the size of the lesion decreased. It has been shown that, in lesions smaller than 2 cm, most HCCs appear as a hypoechoic mass on US (25). The average largest diameter of HCC in our study was 25 mm, which is relatively small, and therefore the hypoechoic pattern may be assumed to be the most common pattern of HCC.

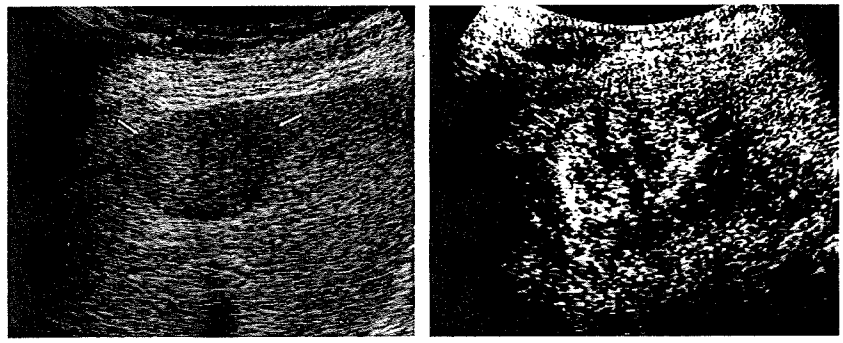

a. b.

Figure 7. A 65-year-old man with metastatic colon cancer *(arrows)*. **(a)** Intercostal B-mode ultrasound shows hypoechoic mass *(arrows)*. **(b)** In the arterial phase, lesion *(arrows)* shows marginal vascularity.

According to the degree of differentiation, there was a tendency that the ratio of the hypoechoic pattern gradually decreased from well-differentiated HCC to poorly differentiated HCC, whereas the thin hypoechoic rim pattern and mosaic pattern, generally specific for HCC, increased from well-differentiated to poorly differentiated HCC. The size of the HCC was assumed to contribute to this trend as well. On the other hand, according to the results of the contrast enhancement pattern of US, most HCCs were classified as diffuse homogeneous (47%) or diffuse heterogeneous patterns (44%).

When the enhancement patterns were examined in tumors other than HCC, including metastatic liver tumor and hemangioma, diffuse patterns were observed in 29% of metastatic liver tumors (most of them showed a diffuse heterogeneous pattern) and 2% of hemangiomas, thus suggesting that this finding would be useful for the differential diagnosis between HCC and other tumors. With regard to the degree of differentiation, 64% of moderately differentiated HCCs showed diffuse homogeneous patterns, whereas 71% and 24% of poorly differentiated HCCs showed diffuse heterogeneous patterns and peripheral nodular patterns, respectively. Thus, the blood distribution within the tumor tended to be more heterogenous in poorly differentiated HCC than in moderately or well-differentiated HCC. However, when the patterns of well-differentiated HCC were compared to those of moderately differentiated HCC, the ratio of a diffuse homogenous pattern to a diffuse heterogenous pattern was slightly lower in well-differentiated HCC than in moderately differentiated HCC, but there were also many nodules that showed similar patterns. Therefore, it is difficult to diagnose the differentiation of HCC even with the arterial-phase information obtained with CEUS.

Jang et al (23) reported that extended observation of the portal phase is helpful in making a correct diagnosis of HCC, because washout later than in the typical portal phase occurs slightly more frequently than does washout within 90 seconds, thus raising the possibility that careful monitoring of not only the arterial phase, but also a relatively late phase could further improve the diagnostic accuracy. Furthermore, newer software developed specifically for CEUS—particularly maximum-intensity-projection techniques—has the potential to improve the diagnostic accuracy in the histologic diagnosis of HCCs (26,27).

Metastatic liver tumors most frequently showed a thick, hypoechoic rim pattern in 42% on baseline US, but also showed various patterns including hypoechoic and hyperechoic patterns. On the other hand, in hemangioma, a hyperechoic pattern (41%) and thin hypoechoic rim pattern (24%), which are generally characteristic of hemangioma, were observed in many cases, but a hypoechoic pattern was also seen in 30%, suggesting that a differential diagnosis with baseline ultrasonographic imaging alone is difficult. However, the thin hypoechoic rim pattern and mosaic pattern, both of which are assumed to be characteristic of HCC, were scarcely observed in metastatic liver tumor and hemangioma and were thus considered useful in the differentiation of these tumors.

According to the classification by contrast enhancement pattern, both metastatic liver tumor and hemangioma tended to show peripheral rimlike and peripheral nodular patterns frequently. Quaia et al (14) reported that most hemangiomas (79%, 44/56) displayed a peripheral nodular pattern; the frequency was higher than that (48%) in our present study. The reason for this discrepancy may be that, although Quaia et al (14) monitored images not only in the arterial phase, but also in other phases in a continuous fashion, we evaluated images only in the arterial phase. In other words, it is possible that hemangioma with a very slow blood flow was diagnosed as having a peripheral rimlike pattern only in the arterial-phase image. Furthermore, it seemed difficult to differentiate between hypovascular-type metastatic liver tumor and hemangioma from images in the arterial phase alone. These may

contribute to the result of CAD analysis demonstrating that the diagnostic accuracy was very high in HCC (98.6%), but was relatively low in hemangioma (93.3%) and metastatic liver tumor (84.8%).

The principal limitation of this study was that almost all specimens for histopathologic diagnosis of the degree of differentiation of HCC were obtained by percutaneous biopsy. The specimens obtained by percutaneous biopsy allowed us to evaluate only a small part of the HCC lesion, which had been produced through a process called multistep hepatocarcinogenesis (ie, successive development of well-differentiated HCC from a dysplastic nodule through a dysplastic nodule with malignant foci), and consequently had histopathologic heterogeneity inside. However, surgical verification is obtained infrequently, especially in patients with HCC, because small HCC lesions are often treated with transcatheter arterial chemoembolization or percutaneous ablation, especially in cirrhotic patients whose functional reserve is severely impaired.

The second limitation is that FNH and hepatic adenoma were not included in this study. Both FNH and hepatic adenoma tend to have FLLs presenting a hypervascular pattern in the arterial phase, and it can be difficult to distinguish from HCC, metastatic liver tumor, and hemangioma. However, Kim et al (28) reported that monitoring the direction of early arterial filling or the vascular morphology continuously by CEUS enables one to differentiate, to some extent, among hepatic tumors with hypervascularity, including FNH, hemangioma, HCCs, or metastases. However, hepatic adenoma lacks characteristic features even with CEUS, and differentiation of hepatic adenoma from other plethoric FLLs has been reported to be difficult. However, hepatic adenoma is a very rare tumor in Japan, and therefore it seems extremely rare for this tumor to become a subject of differential diagnosis.

The third limitation is that current CAD does have information from the images itself rather than criteria that have to be provided subjectively by the physicians. It may be necessary to establish a CAD scheme that recognizes the US images itself automatically as input data. Moreover, to improve the accuracy of diagnosis for FLLs, it would be necessary to use information of not only arterial phase images but also other phase images in the future.

CONCLUSION

We developed a computerized scheme for the classification of focal liver lesions using physicians' subjective classification of echogenic patterns in baseline and contrast-enhanced US. This CAD scheme has the potential to improve the diagnostic accuracy for hepatic lesions, especially for HCC, liver metastasis, and liver hemangioma. However, the accuracy in the histologic differential diagnosis of HCC based on baseline US and CEUS is still limited.

ACKNOWLEDGEMENT

The authors are grateful to Ryo Metoki, MD, Yasuharu Imai, MD, and Liu Guang-Jian, MD, for participating as observers; and to Mrs. Elisabeth Lanzl for improving the manuscript.

REFERENCES

1. Laghi A, Iannaccone R, Rossi P, et al. Hepatocellular carcinoma: detection with triple-phase multi-detector row helical CT in patients with chronic hepatitis. Radiology 2003; 226:543–549.
2. Martin DR, Semelka RC. Imaging of benign and malignant focal liver lesions. Magn Reson Imaging Clin N Am 2001; 9:785–802.
3. Hussain SM, Semelka RC, Mitchell DG. MR imaging of hepatocellular carcinoma. Magn Reson Imaging Clin N Am 2002; 10:31–52.
4. Yamashita Y, Hatanaka Y, Yamamoto H, et al. Differential diagnosis of focal liver lesions: role of spin-echo and contrast-enhanced dynamic MR imaging. Radiology 1994; 193:59–65.
5. Burns PN, Wilson SR, Simpson DH. Pulse inversion imaging of liver blood flow: improved method for characterizing focal masses with microbubble contrast. Invest Radiol 2000; 35:58–71.
6. Harvey CJ, Blomley MJK, Eckersley RJ, et al. Hepatic malignancies: improved detection with pulse-inversion US in late phase of enhancement with SH U 508A-early experience. Radiology 2000; 216:903–908.
7. Huang-Wei C, Bleuzen A, Bourlier P, et al. Differential diagnosis of focal nodular hyperplasia with quantitative parametric analysis in contrast-enhanced sonography. Invest Radiol 2006; 41:363–368.
8. Doi K. Computer status and future potential of computer-aided diagnosis in medical imaging. Br J Radiol 2005; 78(Spec No 1):S3–S19.
9. Doi K. Computer-aided diagnosis in medical imaging: historical review, current status and future potential. Comput Med Imaging Graph 2007; 31:198–211.
10. International Working Party. Terminology of nodular hepatocellular lesions. Hepatology 1995; 22:983–993.
11. Couinaud C. Le foie: etsudes anatomiques et chirurgicales. Paris, France: Masson, 1957; 9–12.
12. Bismuth H. Surgical anatomy and anatomical surgery of the liver. World J Surg 1982; 6:3–8.
13. Itai Y, Ohtomo K, Ohnishi S, et al. Ultrasonography of small hepatic tumors. Radiat Med 1987; 5:14–19.
14. Quaia E, Calliada F, Betolotto M, et al. Characterization of focal liver lesions with contrast-specific US modes and a sulfur hexafluoride-filled microbubble contrast agent: diagnostic performance and confidence. Radiology 2004; 232:420–430.
15. Ashizawa K, MacMahon H, Ishida T, et al. Effect of an artificial neural network on radiologists' performance in the differential diagnosis of interstitial lung disease using chest radiographs. AJR Am J Roentgenol 1999; 172:1311–1315.
16. Abe H, Ashizawa K, Li F, et al. Artificial neural networks (ANNs) for differential diagnosis of interstitial lung disease: results of a simulation test with actual clinical cases. Acad Radiol 2004; 11:29–37.
17. De Gaetano AM, Barbaro B, Chiarla C, et al. The tissue characterization of focal liver lesions by color Doppler echography [in Italian]. Radiol Med (Torino) 1995; 89:453–463.
18. Snow JH Jr, Goldstein HM, Wallace S. Comparison of scintigraphy, sonography, and computed tomography in the evaluation of hepatic neoplasma. AJR Am J Roentgenol 1979; 132:915–918.
19. Becker-Gaab C, zur Nieden J, Sauer U, et al. Sonographic diagnosis of liver tumors: results of comparative studies of ultrasound, computerized tomography, laparoscopy, biopsy and scintigraphy in 413 patients [in German]. Digitale Bilddiagn 1987; 7:35–42.